ISSN 0006-2979, Biochemistry (Moscow), 2007, Vol. 72, No. 7, pp. 683-697. © Pleiades Publishing, Ltd., 2007.
Original Russian Text © E. A. Souslova, D. M. Chudakov, 2007, published in Biokhimiya, 2007, Vol. 72, No. 7, pp. 837-855.

REVIEW

Genetically Encoded Intracellular Sensors Based on Fluorescent Proteins

E. A. Souslova and D. M. Chudakov*

Shemyakin–Ovchinnikov Institute of Bioorganic Chemistry, Russian Academy of Sciences, ul. Miklukho-Maklaya 16/10, 117997 Moscow, Russia; fax: (495) 330-7056; E-mail: ChudakovDM@mail.ru

Received March 13, 2007
Revision received April 9, 2007

Abstract—Green fluorescent protein from *Aequorea victoria* and its many homologs are now widely used in basic and applied research. These genetically encoded fluorescent markers can detect localization of cell proteins and organelles in living cells and also cells and tissues in living organisms. Unique instruments and methods for studies of molecular biology of a cell and high throughput drug screenings are based on fluorescent proteins. This review deals with the most intensively evolving directions in this field, the development of genetically encoded sensors. Changes in their spectral properties are used for monitoring of cell enzyme activities or changes in concentrations of particular molecules.

DOI: 10.1134/S0006297907070012

Key words: genetically encoded sensors, fluorescent proteins, mutant GFP variants, FRET

A family of fluorescent proteins (FP), homologs of green fluorescent protein from *Aequorea victoria* [1], includes hundreds of natural and thousands of mutant variants with various spectral characteristics. These FPs are used in various studies for vital labeling of different objects of molecular biology in studies of the cell. Using a combination of currently available tools [2] based on FP it is possible to monitor the "fate" of a particular cell protein: its expression (promoter activity may be evaluated by expression of corresponding FP gene), localization (using a chimeric construct with FP), motility (using photoactivatable proteins [3-9] and technologies of FP bleaching [10]); interaction with other proteins (using Forster resonance energy transfer (FRET) [11, 12] and split-FP [13]); the rate of degradation (using photoactivatable FP [14] and also timer FP exhibiting time-dependent change in fluorescence [15, 16]).

Abbreviations: BFP) blue fluorescent protein; CaM) calmodulin; CFP) cyan fluorescent protein; EGFP) enhanced green fluorescent protein; EGFR) epidermal growth factor receptor; FLIM) fluorescence lifetime imaging microscopy; FP) fluorescent protein; FRET) Forster resonance energy transfer; GES) genetically encoded sensors; GFP) green fluorescent protein; GKI) protein kinase G; MLCK) myosin light chain kinase; M13) calmodulin-binding fragment of MLCK; PDE) phosphodiesterase; PKA) protein kinase A; TnC) troponin C; YC) Yellow Cameleons; YFP) yellow fluorescent protein.

* To whom correspondence should be addressed.

FPs have been successfully used and are now used as the basis of genetically encoded sensors (GES). They visualize either activity of a protein under study or changes in concentrations of particular molecules. These GES have evident advantages compared with chemically synthesized fluorescent dyes sensitive to certain molecules:

– GES are expressed by cells and therefore they do not require external addition or microinjection. They also do not "leak" out of the cell in the course of a long-term experiment. A stably transfected cell line uniformly expresses GES and this reliably standardizes an experiment;

– employment of signals for intracellular localization directs GES to any particular organelle of living cells;

– it is possible to obtain transgenic organisms expressing GES. Tissue specific promoters can be used to obtain organisms expressing GES in certain tissues. Inducible promoters control expression over time.

Genetically encoded GFP-based sensors can be subdivided into three groups depending on their mode of operation.

The first group of GES includes the FRET-based sensors, using the resonance energy transfer between two variants of FP. Efficiency of energy transfer depends on distance and mutual orientation of two fluorophores. Engineering with two FPs in combination with detector

domains gives a sensor protein that reacts on certain intracellular events by changing its spectral properties.

The second group includes sensors that are built on one molecule of FP (usually its mutated variant) chimerically linked to one, two, or more conformationally active detector domains. Conformational changes or interaction between these domains in response to specific cell signals result in more or less pronounced changes in the structure of such FP, which influence its spectral properties.

The third group includes fluorescent sensors lacking any additional protein domains but sensitive to certain ions due to own intrinsic properties of a sensitized mutant FP. Such sensors were developed for detection of pH values [17-21] and concentrations of chloride [22, 23] and metal ions [24, 25]. However, the list of possible analytes for which this type of GES can be developed is limited by properties of GFP-like proteins. This group of sensors has been reviewed in [26].

In this review we consider the first two groups of GES, which employ specific sensitive protein domains chimerically linked to one or two FPs. Potentially GES can be obtained for any signal molecule or enzyme: this requires use of corresponding protein domains. Thus, development of such sensors is now one of the most promising fields, and many laboratories are working on creating such GES.

CHIMERIC SENSORS BASED ON FRET BETWEEN TWO SPECTRAL VARIANTS OF FLUORESCENT PROTEINS

FRET is the radiationless transfer of energy from an excited donor fluorophore to a suitable acceptor fluorophore. Effective transfer of energy requires overlapping between emission spectrum of the donor and excitation spectrum of the acceptor. FRET also requires close spatial positioning and favorable mutual orientation of the two fluorophores. Energy transfer results in lowering of quantum yield of donor fluorescence and the decrease of its lifetime, the increase of brightness of acceptor fluorescence, and loss of emission light polarization. All these parameters can be measured by the methods of modern fluorescence microscopy [12].

In the simplest (widely used) case, the following parameters are registered in work with FRET indicators: fluorescence intensity of a donor and an acceptor during excitation with light wavelength optimal for donor. Efficiency of resonance energy transfer increases with the decrease in distance between donor and acceptor. This results in the increase in acceptor fluorescence emission and the decrease in brightness of donor fluorescence. Thus, the ratio between brightness of donor and acceptor fluorescence reflects efficiency of FRET between two FPs.

In practice, quantitative measurement of small changes in FRET efficiency is a rather complex task; it requires reasonably good fluorescence microscopy and a set of control samples. It is also important to take into consideration such parameters as possible bleaching of donor or acceptor, their different sensitivity to intracellular parameters (first of all to pH), and possible difference in ratio of donor and acceptor molecules. It is desirable to use spectral microscopy (which effectively decomposes emission spectrum and provides accurate evaluation of FRET efficiency) and also confocal microscopy (which removes signal from out of the confocal plane). There is a widely used method employing acceptor bleaching, which in the presence of FRET is accompanied by the increase in donor brightness [27]. Another method is based on measurement of excitation light depolarization, which depends on the presence and efficiency of FRET [28]. Fluorescence lifetime imaging microscopy (FLIM) is one of the most reliable approaches for quantitative FRET measurement [29, 30], but it requires special equipment that has become widely available only recently.

The main limitation of the FRET-based sensors consists in rather narrow dynamic range (i.e. maximal change in the ratio of donor/acceptor fluorescent signal brightness in response to a specific signal), which is limited by efficiency of energy transfer. Now the maximal dynamic range of FRET-based GES does not exceed 6.6-fold change, and for most sensors this value is just 1.5-2.0-fold (Tables 1-3).

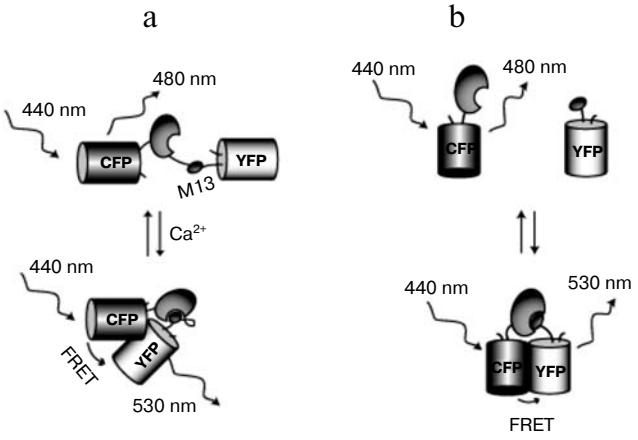

Fig. 1. Scheme of genetically encoded FRET-based sensors. a) The structure of a FRET-based sensor, in which two FPs are covalently linked by detector domains. Yellow Cameleons (YCs) are shown as the example. In calcium-free state, emission of YCs donor fluorophore is observed (maximum at 480 nm). The presence of calcium ions causes calmodulin (CaM) transition into globular form and its interaction with its target peptide M13. This results in closer orientation of FPs (CFP and YFP) accompanied by preferential emission of the acceptor fluorophore (maximum at 530 nm) due to the increase in FRET efficiency. b) The structure of split-variant of the FRET-based sensor. Two variants of FPs (CFP and YFP) are linked to interacting protein domains; association of these domains results in FRET between two approaching fluorophores.

Table 1. Comparative characteristics of FRET-based calcium indicators

Sensor name	Sensitive domain	Donor–acceptor pairs of FP	Maximal contrast *in vitro*, fold	References
FIP-CBsm	MLCK	BGFP/RGFP	↓6	[33]
Cameleon-2	CaM-M13	EBFP/EGFP	↑1.8	[34]
Split Cameleon-2	CaM-M13	ECFP/EYFP	↑>1.8	[34]
Cameleon-3	CaM(E140Q)-M13	EBFP/EGFP	↑1.8	[34]
YC2.0	CaM-M13	ECFP/EYFP	↑1.5	[34]
YC3.0	CaM(E140Q)-M13	ECFP/EYFP	↑1.5	[34]
YC4.0	CaM(E31Q)-M13	ECFP/EYFP	↑>1.5	[34]
YC2.1	CaM-M13	ECFP/EYFP.1(V68L/Q69K)	↑2.0	[34]
YC3.1	CaM(E140Q)-M13	CFP/EYFP.1(V68L/Q69K)	↑2.0	[34]
YC2.3	CaM-M13	ECFP/Citrine	↑2.0	[37]
YC2.6	CaM-M13	ECFP/cp173Venus	↑6.0	[40]
YC3.12	CaM(E140Q)-M13	ECFP/Venus	↑2.0	[40]
YC3.2	CaM(E140Q)-M13	ECFP/cp49Venus	↑1.1	[40]
YC3.3	CaM(E140Q)-M13	ECFP/cp157Venus	↑2.4	[40]
YC3.6	CaM(E140Q)-M13	ECFP/cp173Venus	↑6.6	[40]
YC6.1	CaM-CKKp	CFP/EYFP(V68L/Q69K)	↑2.0	[39]
TN-L15	csTnC	CFP/Citrine	↑2.4	[43]
TN-humTnC	humTnC	CFP/Citrine	↑2.2	[43]
TN-XL	mut csTnC	CFP/cpCitrine	↑5.0	[44]

Note: Maximal contrast of an indicator *in vitro* corresponds to maximal change in the ratio of fluorescence intensities of acceptor versus donor during transition from free to the analyte-bound state. Here and in Tables 2-4, up and down arrows indicate the increase and the decrease in the ratio of fluorescence brightness of acceptor versus donor.

There are two main strategies for the use of the FRET effect between two FPs for detection of intracellular analytes and enzymatic activities. (There are sensors also employing FRET between a fluorescent protein and a synthetic fluorescent dye, buy these are not fully GES and are not considered in this review.) In the first strategy, the donor/acceptor couple of FPs is covalently linked via a detector domain (or domains), undergoing structural changes in response to modification by a cell enzyme or to interaction with analyte (Fig. 1a). Advantage of such "classical" FRET sensors consists in the presence of equimolar quantities of donor, acceptor, and detector domains. Another advantage is that when using a sensor with two interacting domains, these domains preferentially exhibit intramolecular interaction. Thus, all active molecules of such a sensor contribute to final changes of brightness and, consequently, in the dynamic range detected in living cells *in vivo*. On the other hand, spatial approach of both fluorophores within one chimeric construct causes appearance of background FRET signal even in the absence of detected analyte or enzymatic activity, and this may decrease the dynamic range of such indicators [31].

The second strategy involves the attachment of donor and acceptor fluorophores to separate domains (Fig. 1b). Interaction of these domains causes closer orientation of FPs and appearance of FRET between them. Such split variants of the FRET-based biosensors are used for visualization of intermolecular interaction. However, the detector domains may also interact with unlabeled endogenous components. Such interaction does not cause donor/acceptor approach and FRET does not appear. This effect may decrease the dynamic range of the signal detected in living cells compared with results obtained for the same sensor *in vitro*. The decrease in the dynamic range can also be determined by different level of expression of two FPs [31]. On the other hand, lack of background FRET in the absence of interaction of detector domains is an evident advantage of such sensors. Such indicators exhibit better localization in particular organelles, and they rarely form abnormal aggregates.

Below we consider the main types of known FRET-based sensors, which have been classified by detected analyte or enzymatic activity.

FRET-based calcium biosensors. During recent decades, the creation of calcium-sensitive indicators has

Table 2. Comparative characteristics of FRET-based indicators of cyclic nucleotides and sensors of G-protein activity

Sensor name	Target	Sensitive domain	Donor–acceptor pairs of FP	Maximal contrast *in vivo*, fold	References
FRET-based indicators of cAMP					
Split indicator of cAMP	cAMP	Cat PKA, IIβ Reg PKA	CFP/YFP	↓	[46]
FRET-based indicators of cGMP					
CGY-Del1	cGMP	GKIΔ1-47	BGFP/RGFP	↑ 1.2-1.5	[48]
Cygnet-2	cGMP	GKIΔ1-77(T516A)	ECFP/EYFP	↓ 1.4-1.5	[47]
cGES-GKIB	cGMP	B-domain GKI	CFP/YFP	↓ 1.2	[49]
cGES-DE2	cGMP	GAF-domain PDE2A	CFP/YFP	↑1.4	[49]
cGES-DE5	cGMP	GAF-domain PDE5A	CFP/YFP	↑ 1.4	[49]
FRET-based sensors of G-protein activity					
Raichu-Ras	Ras	Ras, RBD-domain Raf1	CFP/YFP	↑ 2.0	[51]
Raichu-Rap1	Rap1	Rap1, RBD-domain	CFP/YFP	↑ 2.0	[51]
Raichu-Cdc42	balance GEFs/GAFs Cdc42	CRIB-domain PAK1, Cdc42	YFP/CFP	↑	[52]
Raichu-Rac1	balance GEFs/GAFs Rac1	CRIB-domain PAK1, Rac1	YFP/CFP	↑	[52]
Raichu-CRIB	GTP-Rac/GTP-Cdc42, RhoGDIs	CRIB-domain PAK1	YFP/CFP	↓	[52]
Cdc42-indicator	Cdc42	CRIB-domain WASP	YFP/CFP	↓ < 3.2	[54]
Cdc42-GEFs-indicator	Cdc42-GEFs	CRIB-domain WASP	YFP/CFP	↓ < 1.7	[54]
Raichu-RhoA	balance GEFs/GAFs RhoA	RhoA(1-189), RBD-domain PKN	YFP/CFP	↑	[55]
Raichu-RBD	GTP-RhoA, RhoGDIs	RBD-domain Rhotekin	YFP(L222K/F224R)/CFP	↓	[55]

become especially important. Cells employ calcium as a second messenger in regulation of numerous intracellular processes including differentiation, apoptosis, secretion, neurotransmitter release, learning and memory, and also muscle contraction and behavior of some ion channels [32]. Fluctuations of calcium concentrations regulate behavior of chaperons responsible for posttranslational protein folding. The increase in cytosolic calcium in a neuron within a few milliseconds after membrane depolarization makes calcium indicators irreplaceable reporters of rapid neuronal activity.

FIP-CBsm was the first FRET-based calcium biosensor [33]. Two mutant GFP variants, blue fluorescent protein (BFP; maximum emission at 440 nm) and optimized red-shifted green fluorescent protein (RSGFP, single maximum of fluorescence excitation and emission at 480 and 505 nm, respectively), were linked by calmodulin binding fragment of myosin light chain kinase (MLCK). In the absence of calcium ions, excitation of the BFP chromophore at 380 nm causes bright fluorescence emission of RSGFP due to effective FRET between the two FPs. The biosensor functioning is based on activity of endogenous CaM, the most abundant calcium-binding protein expressed in all eukaryotic cells. Regulating activity of numerous protein targets (protein kinases, phosphatases, adenylate cyclases, phosphodiesterases, Ca^{2+}-ATPase, cytoskeleton proteins, etc.), CaM is involved in regulation of such cell processes as endo- and exocytosis, glycogenolysis and lipolysis, tubulin polymerization, and also neurotransmitter secretion.

Table 3. Comparative characteristics of FRET-based indicators of kinase activity

Sensor name	Target	Sensitive domain	Donor–acceptor pairs of FP	Maximal contrast *in vivo*, fold	References
ART	PKA	KID-domain of CREB-substrate	BGFP/RGFP	↓ 1.22	[59]
AKAR1	PKA	substrate PKA, 14-3-3τ	ECFP/Citrine	↑ 1.25-1.50	[60]
Srk-indicator	Src	substrate Srk, SH2-domain	ECFP/(EYFP or Citrine)	↓ 1.25-1.30	[61]
EGFR-indicator	EGFR	substrate EGFR, SH2-domain	ECFP/(EYFP or Citrine)	↑ 1.25-1.35	[61]
Abl-indicator	Abl	substrate Abl, SH2-domain CrkII	ECFP/(EYFP or Citrine)	↑1.15-1.30	[61]
Picchu	Abl/EGFR	CrkII (SH2-SH3-SH2) del	CFP/YFP	↑ 1.60	[62]
Aktus	Akt/PKB	substrate Akt/PKB, 14-3-3η	CFP/YFP	↑ 1.10	[74]
BKAR	Akt/PKB	substrate Akt/PKB, FHA2-domain Rad53p	mCFP/mYFP	↓ 1.10-1.25	[63]
CKAR	PKC	substrate PKC, FHA2-domain Rad53p	mCFP/mYFP	↓ 1.15-1.20	[64]
EAS-2	ERK2	mEtsI(15-46)	ECFP/EYFP	↓	[65]
EAS-3	ERK2	hElkI(375-404)	ECFP/EYFP	↓	[65]
EAS-5	ERK2	hElkI(360-419)	ECFP/EYFP	↓	[65]

Note: Maximal contrast of an indicator *in vivo* corresponds to maximal change in the ratio of fluorescence intensities of donor versus acceptor during phosphorylation of substrate domain of a sensor compared with the non-phosphorylated state.

Interaction of calcium-bound CaM with the MLCK fragment of this biosensor caused spatial separation of BFP and RSGFP accompanied by lowered efficiency of FRET between them. This caused simultaneous decrease in intensity of acceptor RSGFP emission and the increase in intensity of donor BFP emission. In the case of FIP-CBsm, there was a 6-fold change in the ratio of fluorescence intensity of the two FPs during transition from calcium free into calcium-bound state *in vitro*. However, low photostability of BFP is a significant shortcoming of this sensor.

More recently, other FRET-based calcium biosensors (called "Cameleons" due to the presence of CaM domain and their ability to change color) have been developed [34]. Cameleons contain two mutant GFP variants (BFP and EGFP (enhanced green fluorescent protein)) linked by sequentially positioned domains of CaM and its target peptide M13 (the fragment of MLCK). Yellow Cameleons (YC) employ a CFP/YFP (cyan fluorescent protein/yellow fluorescent protein) couple. In contrast to FIP-CBsm, the interaction of Cameleons causes increase in FRET between two GFP mutants due to conformation change in the linker module. Binding of four calcium ions changes CaM conformation from extended propeller-like shape into a compact globule; this results in CaM interaction with M13 and approaching of the two fluorophores (Fig. 1a). The chimeric construct CaM-M13 (without FPs) exhibits biphasic kinetics of Ca binding with two K_d values of 2 μM and 80 nM. This is attributed to independent binding of calcium ions to N- and C-terminal domains of CaM, respectively [35]. Cameleons exhibit similar biphasic dependence of calcium ion concentration with corresponding K_d values of 11 μM and 70 nM [34].

Since the appearance of the first Cameleon biosensor in 1997, many additional versions have been engineered [36-40]. The original version of Cameleon employs blue (BFP) and green (GFP) mutants as donor and acceptor, respectively, whereas in Yellow Cameleons (YCs) FRET occurs between CFP and YFP [36]. Substitution of donor BFP for CFP increased fluorescence brightness and signal/noise ratio (cell auto-fluorescence). However, in contrast to the initial Cameleon version, *in vitro* the YCs are characterized by lower dynamic range (of 1.8- and 1.5-fold for EBFP/EGFP and ECFP/EYFP, respectively). Acceptor EYFP also increased pH sensitivity of YCs and their susceptibility to the effects of reversible photoconversion at high irradiating light intensity [36].

Depending on the YC CaM affinity to calcium, the Cameleons can be subdivided into several groups. For example, the biosensors of YC2 subgroup contain intact

CaM domain with maximal affinity for calcium ions. In YC3 and YC4 FRET-based biosensor series affinity for calcium was decreased by two point mutations (E140Q and E31Q, respectively) in the calcium-binding loop of the CaM domain [36].

In the initial YC version, fluorescence of acceptor EYFP strongly depended on pH. Under alkaline and acidic pH values EYFP fluorescence was unstable and imitated a decrease in calcium concentration. The improved versions, YC2.1 and YC3.1, containing EYFP.1 (V68L/Q69K) instead of EYFP, were able to detect fluctuations of calcium concentrations without pH-inducible changes in the range of pH from 6.5 to 8.0 [36].

Recently new YC versions have been developed; they are based on brighter and more pH stable yellow fluorescent proteins Citrine [37] and Venus [41], which are effectively matured at 37°C. Later red Cameleons [38] have been obtained by substitution of the acceptor for DsRed (red fluorescent protein from *Discosoma* coral) [42].

Substitution of EYFP.1 in YC3.1 with permuted variants of yellow FP Venus (cpVenus) resulted in YC3.2-YC3.9 sensors with altered characteristics [40]. For example, YC3.6 (based on cp173Venus) was characterized by the record 6.6-fold dynamic range (versus 2-fold dynamic range in the initial YC3.1).

The sensor YC6.1 was developed to increase FRET efficiency *in vivo* [39]. In the preceding YC2.1 sensor, CaM-binding peptide M13 (MLCKp) was linked to the C-end of CaM [36]. In YC6.1, the CaM-binding peptide (CKKp) was inserted between N- and C-terminal domains of CaM. In contrast to YC2.1, exhibiting biphasic curve of calcium binding (with corresponding K_d values of 100 nM and 4.3 μM), YC6.1 is characterized by a monophasic curve with a single K_d value of 110 nM. However, in spite of lower maximal dynamic range and slow activation kinetics, this sensor exhibited a 2-fold increase in the FRET signal *in vivo* in the range of physiological concentrations of calcium from 0.05 to 1 μM (in the case of YC2.1 there was 1.4-fold contrast) [36, 39].

Heim and colleagues [43] generated FRET-based calcium biosensors employing troponin C (TnC), the regulator of contractions of skeletal and myocardial muscle; its major advantage consists in minimal interaction with intracellular biochemical environment. By analogy with related "Cameleons", the generation of the FRET-based calcium biosensor employing TnC was named S-Troponeon ("S" for skeletal TnC in TN-L15) and C-Troponeon ("C" for cardiac TnC in TN-humTnC) [43]. In these sensors two FPs (CFP and Citrine) are linked together by a calcium-binding moiety (TnC), changing its conformation in the presence of calcium ions. The S-Troponeon sensor named TN-L15 employs chicken TnC partially truncated at its N-end (csTnC) as a linker for CFP and Citrine. Calcium binding to the sensor linker domain containing TnC caused its compactization and thus increased efficiency of FRET between flanking FPs. The dynamic range for TN-L15 was 2.4-fold *in vitro*. Insertion of human cardiac TnC between CFP and Citrine resulted in the development of TN-humTnC sensor with 2.2-fold dynamic range *in vitro*. The K_d values for TN-humTnC and TN-L15 were 470 nM and 1.2 μM, respectively [43].

In 2006 improved versions of FRET-based calcium biosensors employing TnC appeared. The sensor named TN-XL was developed by engineering magnesium and calcium-binding properties within the C-terminal lobe of TnC and simultaneous substitution of yellow fluorescent protein Citrine with its permuted variant cpCitrine. There was a 5-fold dynamic range for TN-XL biosensor *in vitro*. This sensor shows linear response of FRET efficiency over calcium concentration and high stability to physiological range of pH changes [44].

FRET-based sensors of cyclic nucleotides. The cyclic nucleotides cAMP and cGMP are intracellular second messengers that are involved in signal transduction from hormones (e.g. glucagon, adrenaline, or peptide hormones) to effector proteins. cAMP activates protein kinase A (PKA) and controls numerous cell processes including glycogenolysis (glycogen breakdown), lipolysis, and calcium transport via ion channels. cGMP activates protein kinase G (GKI), regulates phosphodiesterase (PDE) behavior, ion channel conductivity, neuron excitability, apoptosis, and smooth muscle tone. cGMP also plays a central role in vision in mammals [45].

Until recently it was not possible to monitor changes in cAMP concentrations, and this complicated understanding of its role in signal transduction in living cells. Engineering genetically encoded fluorescent cAMP biosensors allowed direct monitoring of intracellular cAMP level.

One of the first cAMP indicators was a slit-variant of the FRET-based biosensor (Fig. 1). It consists of catalytic subunit of cAMP-dependent PKA and IIβ isoform of its regulatory subunit; these subunits are linked to YFP and CFP, respectively. Both parts of this biosensor were transfected into rat cardiomyocytes; stimulation of β-adrenergic receptors of these cells was accompanied by activation of adenylate cyclase. Binding of cAMP to the regulatory subunit of PKA induced dissociation of PKA subunits accompanied by impairment of FRET. Thus, the decrease in the FRET signal showed the increase in cAMP level in living cells [46].

Based on information that α-isoform of protein kinase G (GKIα) undergoes significant cGMP-dependent conformational changes, two research groups independently developed FRET-based cGMP biosensors. They inserted partially deleted undimerized mutants of GKIα between two FPs [47, 48]. Binding of cGMP caused transition of closed (compact) conformation of GKIα into opened extended conformation. Both groups suggested that in the presence of cGMP their sensors

would be characterized by a decrease in FRET efficiency. However, the behavior of the two sensors unexpectedly differed.

CGY sensors [48] contain a partially deleted fragment of cGMP-dependent protein kinase G (Δ1-47 GKI) between two GFP mutants (BGFP/RGFP). Binding of cGMP to such CGY biosensor caused up to 1.5-fold increase in FRET efficiency *in vitro*.

In the Cygnet sensors [47] two other FPs (ECFP/EYFP) were linked with GKI fragment (Δ1-77) with deleted kinase activity. In the case of Cygnet-2, there was 1.4-1.5-fold dynamic range *in vitro*. However, it was opposite to the change in fluorescence compared with CGY sensors: there was cGMP-dependent decrease in FRET efficiency. Application of CGY- and Cygnet-biosensors was limited by their narrow dynamic range in living systems and also low specificity [47, 48].

A recent study [49] has demonstrated development and application of new variants of cGMP sensors based on GKI and PDEs. In contrast to two previous studies employing GKI variants with several functional domains, Nilolaev and coworkers employed only nucleotide binding B-domain of GKI or regulatory GAF-domain of PDEs. GAF-domains present in cGMP-dependent PDEs mediate cyclic nucleotide effect on catalytic activity of these enzymes. In the sensors containing GKI B-domain (e.g. cGES-GKIB), cGMP binding decreased FRET efficiency between CFP and YFP, whereas in the case of constructs containing PDE (e.g. cGES-DE2 and cGES-DE5) cGMP binding was accompanied by increased efficiency of FRET between CFP and YFP.

Comparison of affinities of the described cGMP sensors revealed that the CGY biosensor exhibits the highest affinity for cGMP (K_d = 20 nM), the affinity of the other sensors varying in the micromolar range. However, the CGY biosensor had the lowest selectivity for cGMP (versus cAMP), which was less than 10-fold. Other biosensors were characterized by much higher selectivity of 100-fold (cGES-GKIB and cGES-DE2) and even 400-600-fold (cGES-DE5 and Cygnet) [47-49].

Thus, the construct cGES-DE5 seems to be the most preferable cGMP biosensor. It has good spatial and time resolution and also higher selectivity to cGMP than cGES-GKIB and Cygnet. The two latter sensors exhibit slower kinetics of cGMP binding, which is determined by properties of its constituent, GKI B-domain, and therefore they cannot visualize rapid fluctuations of intracellular cGMP concentrations [49].

FRET-based sensors of G-protein activity. Use of fluorescent GES plays an important role in studies of intracellular signaling involving G-proteins. In living cells, these G-proteins cycle between inactive (GDP-bound) and active (GTP-bound) states. The transition between these two states is regulated by guanine nucleotide exchange factors (GEFs) and GAP proteins (GAPs) activating GTPase activity of G-proteins. Signal cascades involving G-proteins provide biological response to various stimuli, which include hormones, odorants, neurotransmitters, etc. G-Proteins of Ras-GTPase superfamily function as molecular switches for many cell signals. GTPases of Rho family (Rac1, Rho, and Cdc42) are involved in regulation of a wide spectrum of cell functions such as membrane transport, activation of transcription, cell cycle progression and cytokinesis, and also actin cytoskeleton modeling during cell migration, phagocytosis, etc.

All genetically encoded FRET-based sensors of GTPase activity can be subdivided into three types: 1) split variants of FRET-based sensors (Fig. 1); 2) FRET-based sensors containing the sensitive module "GTPase–effector domain"; 3) FRET-based sensors containing only an effector domain located between two FPs. Figure 2 schematically shows sensors of G-protein activity of the second and third types.

Janetopoulos et al. [50] described the FRET-based spit sensor, which could visualize changes in activity of GTP-binding proteins (G-proteins) in *Dictyostelium discoideum* cells. The detected parameter was the FRET level between cyan and yellow FPs covalently attached to α- and β-subunits of G-protein. Association of tagged Gα and Gβ with endogenous Gγ-subunit into a heterotrimer was accompanied by effective energy transfer

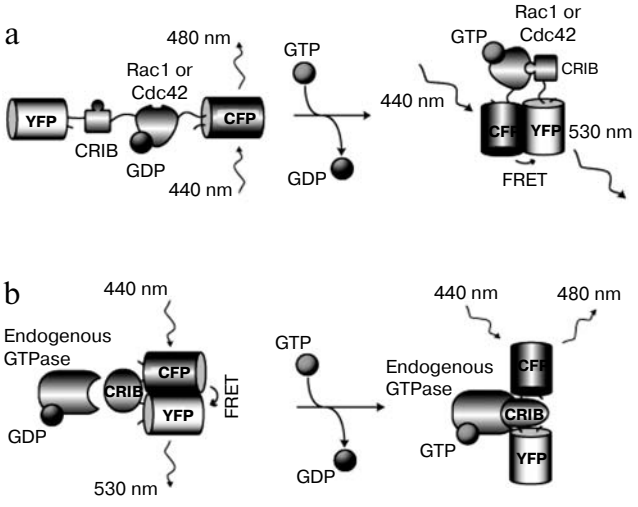

Fig. 2. Scheme of genetically encoded sensors for GTPase activity. a) Raichu-Rac/Cdc42 sensors constructed on the basis of the "GTPase–effector domain" module. Intramolecular binding of GTP-activated form of Rac1/Cdc42-GTPase with CRIB-domain brings together the two FPs and increases FRET efficiency between them. b) In the Raichu-CRIB sensor two FPs are linked by one effector domain (CRIB). In the inactive (GDP bound) form two sensor FPs are closely positioned, and this causes preferential emission of acceptor fluorophore (YFP) due to effective FRET. During activation of Rho-dependent signaling pathway the sensor CRIB domain binds endogenous Rac/Cdc42-GTP, undergoes conformational changes, and this causes spatial separation of the two FPs and termination of FRET.

between the two approaching fluorophores. Dissociation of heterotrimer terminated FRET.

Sensors for activity of Ras family GTPases, possessing the common name Raichu (**R**as **a**nd **i**nteracting protein **ch**imeric **u**nit), employ Ras-binding domain of Raf1 effector (RBD); it binds the activated (GTP-bound) form of Ras 10,000 times more effectively than inactive GDP-bound form. Raichu sensors of the second and third types employ the sensitive module "GTPase–effector domain" as the linker domain between two FPs (Fig. 2). Since the effector domain of GTP bound form of Raichu is engaged in interaction with RBD domain, this sensor does not influence intracellular signaling by binding protein targets. However, Raichu sensors have some shortcomings. First of all, they detect local intracellular concentrations of GEFs and GAPs capable of interaction with the sensor RBD and change its properties rather than activation of Ras protein itself. Second, most Raichu-type sensors are insoluble during expression in bacterial systems and a detectable signal could be obtained only in strains of eukaryotic cells characterized by its increased expression. Third, the level of expression of Raichu sensor with membrane localization is significantly lower compared with its cytoplasmic version, and therefore it is not easy to get high value of signal/noise ratio especially on activation of a limited fraction of this sensor.

Mochizuki and coauthors developed Raichu sensors for monitoring activation of Ras and Rap1 GTPases in living cells. Chimeric constructions Raichu-Ras/Raichu-Rap1 share some similarity with Cameleons calcium sensors described above. They consist of GTPase (Ras and Rap1) and RBD (Ras-binding domain of Raf1), flanked by two mutant GFPs of the following sequence: YFP-Ras-RBD-CFP. In the inactive GDP-bound state of the indicator, YFP and CFP are spatially separated; this results in preferential emission of the donor fluorophore (CFP). During activation of the Ras signaling pathway the GDP-bound form of the sensor GTPase is transformed into the GTP-bound form. This results in RBD binding of Ras-GTP followed by reversible approach of YFP and CFP and the increase in FRET efficiency between them. The indicators Raichu-Ras and Raichu-Rap1 were co-expressed in HEK-293T cells with GEFs or GAFs of the Ras-family GTPase. The highest changes in the FRET signal (up to 2-fold increase in the efficiency of FRET in the GTP-bound form of the sensor versus GDP-bound form) were obtained *in vivo* in the presence of GEFs. Thus, Raichu-Ras and Raichu-Rap1 can be employed for monitoring of corresponding G-proteins in living cells [51].

Itoh et al. [52] developed FRET indicators for monitoring local balance of GEFs and GAFs Rac1- and also Cdc42-GTPase activities in membrane compartments of living cells. They were named Raichu-Rac and Raichu-Cdc42. These indicators contain PAK1 (CRIB), GTPase-binding domain, Rac1- or Cdc42-GTPase, and two FPs (YFP and CFP). The membrane localization signal (Ki-Ras CAAX motif) was attached to the C-end of the chimeric construct. Intramolecular binding of GTP-activated form of Rac1 (or Cdc42) with CRIB-domain caused closer proximity of the two FPs and increased FRET efficiency. However, in contrast to Raichu-Ras sensors, there was reverse order of positions of GTPase and the effector domain (CRIB-GTPase) in the Raichu indicators of the Rho-family of GTPases.

Besides GEFs and GAPs, the members of Rho-family of GTPases are also regulated by guanosine dissociation inhibitors (GDIs). GDIs not only compete with GEFs but also determine cytoplasmic localization of Rho-GTPase. Thus, dissociation of GDI from Rho-GTPase causes enzyme activation and its association with membrane. Rho GDIs recognize isoprenoid C-terminal site of Rho-GTPase [53]. Since the effector domain of Raichu-Rho indicators is attached to the C-end of GTPase and CAAX motif facilitating farnesylation and acting as the membrane localization signal is positioned at the C-end of the whole chimeric construction, such indicators do not recognize Rho GDIs.

For solution of this problem the Raichu-CRIB sensor has been developed. It belongs to the third type of GTPase activity indicators (based on one effector domain only). In this case, only the CRIB GTPase binding domain was positioned between YFP and CFP (Fig. 2). The Raichu-CRIB sensor was co-expressed in HEK-293T cells with constitutively activated Rac1- or Cdc42-GTPase. Interaction between GTP-Rac1/GTP-Cdc42 with the sensor CRIB decreased interaction between YFP and CFP and reduced FRET between them. Thus, Raichu-CRIB detected local intracellular concentrations of GTP-bound Rho-GTPases and activity of Rho GDIs. However, its expression impaired endogenous Rac and Cdc42 signal cascades and Raichu-CRIB exhibited low specificity. It was shown that this sensor interacted with both Rac1 and Cdc42. This complicated interpretation of the fluorescent response. It should be noted that in the Raichu-CRIB the signal/noise ratio was lower than for Raichu indicators containing GTPase effector domain module [52].

Cdc42 GTPase induces significant conformational changes in the WASP protein (Wiskott–Aldrich syndrome protein). Seth and coauthors developed their own series of indicators of Cdc42 and Cdc42-GEFs activities; these indicators of the third type were based on WASP CRIB domain positioned between YFP and CFP [54]. *In vitro* decrease in FRET efficiency for this Cdc42 indicator reached 3.2-fold upon binding of activated GTP bound form of Cdc42. During GDP exchange for GTP, the Cdc42 GEFs sensors demonstrated a 1.7-fold change in FRET signal. Although *in vivo* both sensors reliably detected changes in Cdc42 and Cdc42-GEFs activities, they were characterized by low specificity [54].

Following the design procedure described earlier for indicators of Ras superfamily GTPase, Yoshizaki and

coauthors developed two new sensors for monitoring of RhoA GTPase activity; they were named Raichu-RhoA and Raichu-RBD [55]. The Raichu-RhoA sensor contained partially deleted form of RhoA GTPase and RhoA binding domain (RBD) of effector PKN protein flanked by YFP and CFP. In the presence of GTP, RBD interacted with RhoA and this increased FRET efficiency between the two fluorophores.

The indicator Raichu-RBD (similar to the described above Raichu-CRIB [52]) was developed for detection of activity of Rho GDIs by monitoring of endogenous level of GTP-RhoA. This indicator contained YFP, RBD of the effector Rhotekin protein, and CFP. It was shown that FRET efficiency in Raichu-RBD reflected total amount of GTP-RhoA, rather than a ratio of its GTP/GDP bound forms. Low FRET efficiency corresponded to high level of RhoA activity. However, Raichu-CRIB exhibited low specificity with respect to various members of Rho GTPases [55].

In conclusion of this section, we should say that none of the GES can give exhausting information about spatio-temporal activity of intracellular GTPases. Three types of GTPase sensitive FRET indicators have been developed. The first one represents the split variant of the FRET sensitive system. The second type of GTPase sensors can monitor ratio of activities of GEFs and GAFs regulators, whereas the third type of sensors detect the presence of activated GTP-bound GTPase (Table 2).

FRET-based sensors for kinase activity. Study of intracellular pathways of signal transduction is one of the most intensively developing fields of modern science. Complexity and specificity of numerous pathways of signal transduction require spatial microcompartmentalization of kinase and phosphatase activities.

Various methods have been used for visualization of kinase activity *in situ*, including fluorescently labeled antibodies recognizing phosphorylation sites [56, 57] or microinjections of the fluorescently labeled substrates of kinases [58]. However, these methods require fixation and microinjections and give insufficient spatial or temporal resolution, i.e. they cannot give real-time monitoring of kinase activity in living cells. Thus, visualization of kinase activity (as well as oscillations of intracellular concentrations of calcium ions) required development of a new generation of genetically encoded indicators. Most GES for kinase activity employ the FRET mechanism. Such sensors consist of two fused FP variants linked together by means of kinase peptide substrate and phosphoamino acid binding domain. Phosphorylation of a substrate induces formation of intramolecular complex between the substrate and the recognizing domain. Resulting conformational rearrangements influence FRET efficiency between flanking FPs.

Monitoring of PKA present in all mammalian cells and involved in numerous parallel signaling cascades attracts special interest.

In 2000, Nagai and coauthors [59] developed a genetically encoded FRET sensor named ART (c**A**MP-**r**esponsive **t**racer). This sensor detected phosphorylating activity of PKA *in vivo* [59]. In this sensor, two fused GFP mutants (BFP and YFP) were linked via kinase induced domain (KID) of the transcription factor CREB (**c**AMP-**r**esponsive **e**lement **b**inding protein). cAMP stimulates PKA, which phosphorylates KID domain. The latter undergoes significant conformational changes in response to phosphorylation. In the ART sensor, these conformational changes cause a decrease in FRET efficiency between flanking FPs. Thus, the decrease in intensity of FRET signal in the ART indicator suggests the increase in PKA activity in mammalian cells [59].

The other sensor of PKA activity, named AKAR1, consists of CFP, phosphoamino acid binding domain 14-3-3τ, a consensus substrate of PKA, and the yellow FP Citrine. Phosphorylation of the peptide substrate of the AKAR1 sensor by PKA results in formation of its intramolecular complex with 14-3-3τ. This increases the FRET efficiency between the two fluorophores due to changes of their mutual orientations and closer spatial proximity. Dephosphorylation of the substrate peptide by phosphatase returns FRET to its initial state. Stimulation of HeLa cells expressing the AKAR1 indicator with forskolin (Fsk) (adenylate cyclase activator) caused 1.25-1.5 increase in FRET efficiency [60].

Ting et al. [61] described three GESs for activities of Src and Abl kinases and epidermal growth factor receptor (EGFR). These tyrosine kinases are the key components of two different signaling pathways activated by growth factors. All three of the indicators consist of sequentially linked modules: CFP, phosphotyrosine binding domain SH2, a consensus substrate for the corresponding kinase, and YFP. Kinase induced the same changes in FRET efficiency that were considered above for the AKAR1 sensor. Growth factor stimulation of activity of one of three kinases (Src, Abl, or EGFR) in living cells expressing corresponding indicator caused 1.2-1.35-fold changes in their FRET signal. The EGFR and Abl indicators reacted on phosphorylation by corresponding kinases with increase in FRET efficiency, whereas phosphorylation of the Src sensor decreased FRET. The specificity of each indicator was tested *in vitro* using a set of various kinases. It was demonstrated that the EGFR indicator was phosphorylated by EGFR kinase, but it did not react on Abl, Src, and Lck kinases, and also on serine/threonine MAP-kinase ERK1. The Ab1 sensor was specifically phosphorylated by Abl and EGFR. The Scr indicator exhibited the lowest specificity of these three sensors. It exhibited detectable signal in response to phosphorylation by Src, Abl, Lck, and EGFR kinases. Data on Abl sensor (based on SH2 domain of CrkII) [61] are consistent with results obtained using a Picchu indicator described in an independent study [62].

The Picchu sensor (**p**hosphorylation **i**ndicator of **C**rkII **ch**imeric **u**nit) consists of CrkII protein, positioned

between yellow and cyan FPs (YFP and CFP). The adaptor CrkII protein, which consists of one SH2 and two SH3 domains, is involved in various cell processes, including apoptosis, growth, and migration of cells. Growth factor stimulation (e.g. EGF) causes CrkII phosphorylation; this induces intramolecular binding of SH2 domain with phosphotyrosine. Kurokawa and colleagues [62] used this property of CrkII to change its conformation in response to phosphorylation for the development of the Picchu indicator. In this indicator, phosphorylation caused closer proximity of CFP and YFP accompanied by the increase in FRET efficiency between them. Partial deletion of CrkII at its C-end resulted in appearance of new versions of Picchu characterized by increased dynamic range. The sensor Picchu-X contains Ki-Ras CAAX motif at its C-end. Picchu-X expressed on plasma membrane is characterized by increased sensitivity and temporal resolution. However, it should be noted that Picchu-X can detect only "output" signal of CrkII phosphorylation, whereas a cytoplasmic version of Picchu reflects total level of CrkII phosphorylation [62].

Sasaki and coworkers developed a FRET sensor named Aktus for detection of Akt/protein kinase B (PKB) activity [63]. Akt/PKB is a serine/threonine protein kinase that shares homology with PKA and PKC. Akt is activated in response to various stimuli, including growth factors, cytokines, steroid hormones, and cell stress; it plays a key role in regulation of cell survival, insulin signaling pathway, and oncogenesis. Aktus consists of two FPs (CFP/YFP), a specific phosphorylation substrate for Akt/PKB, a flexible linker, and the domain 14-3-3, which recognizes phosphorylated form of the substrate. In the case of cytoplasmic localization of the indicator, phosphorylation was not visualized, whereas expression of its versions in Golgi complex and mitochondria (by means of specific targeting signals) exhibited detectable changes of FRET in response to phosphorylation. Differences in results obtained using these three versions of such indicator can be attributed to localization of Akt kinase in subcellular compartments such as mitochondria and Golgi complex.

Another FRET indicator of Akt/PKB kinase activity named BKAR (**B k**inase **a**ctivity **r**eporter) was described in [64]. In contrast to Aktus, the BKAR indicator employed an artificially designed peptide, and FHA2 domain of yeast Rad53p. FHA2 was characterized by moderate affinity to the phosphorylated form of the peptide substrate and reversibly bound it. Thus, it was possible to visualize kinase activity of endogenous PKB and detect termination of signal PKB-dependent pathway during PKB inhibition.

The BKAR structure is similar to earlier developed indicator of PKC activity named CKAR (**C k**inase **a**ctivity **r**eporter) [65]. The only difference consists in composition of a peptide substrate, adapted in each case for phosphorylation by a certain protein kinase. In the non-phosphorylated state BKAR (as well as CKAR) has a conformation that favors FRET between CFP and YFP. Phosphorylation of threonine residue of the sensor peptide substrate of these indicators caused structural rearrangements resulting in decreased FRET efficiency [64, 65].

Green and Alberola-Ila [66] described FRET sensors for detection of MAP kinase activity; they were named EASs (**E**RK **a**ctivity **s**ensors). It was shown that after phosphorylation by ERK-2 kinase *in vitro* the EAS indicators demonstrated various changes in FRET signal between ECFP and EYFP. These changes depended on composition of ERK-specific phosphorylation substrate linking the FPs in the various indicators. The sensor EAS-2 contained a fragment of human transcription factor EtsI; EAS3-5 employed a sequence of human ElkI. All EAS variants reacted on phosphorylation by ERK2 with a decrease in FRET efficiency. The sensor EAS-3 (based on ElkI) was characterized by highest ERK2-dependent change in FRET signal (Table 3).

CHIMERIC SENSORS BASED ON A SINGLE FP MOLECULE

This group of GES often employs a **c**ircularly **p**ermuted **f**luorescent **p**rotein (cpFP). Permuted proteins are such protein variants in which their N- and C-termini are joined together by genetic engineering methods and peptide linkers, and new N- and C-termini are formed in another part of the protein molecule. The nomenclature of the permuted proteins is based on the positions of a polypeptide chain where new N- and C-termini are located (e.g. cpEGFP 149-144) (Fig. 3).

Based on stability of β-barrel structure of FP and posttranslational modification required for formation of its chromophore, it was relevant to suggest that rearrange-

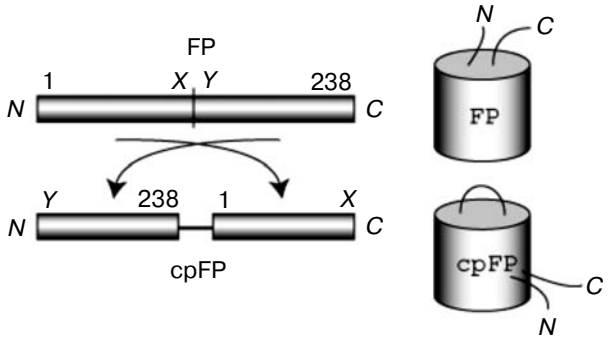

Fig. 3. Scheme illustrating circular permutation of a fluorescent protein. *X* and *Y* designate breakpoints used for permutation. The right part schematically shows β-barrel of initial fluorescent protein (FP) and its permuted version (cpFP). The breakpoint was introduced near a cpFP chromophore, and native N- and C-termini were joined together with a peptide linker.

ments of insertions into FPs would impair their fluorescence. Nevertheless, it was demonstrated that some FPs "survived" after permutation and certain positions were tolerant to insertion of the whole detector proteins. If an inserted protein is a conformationally sensitive receptor, binding of its ligand may significantly influence FP fluorescence [67, 68]. These studies stimulated the development of a new type of GES.

Permutation allows placement of sensitive domains in a close proximity to a protein chromophore. In this case, conformational changes in the detector domains cause marked structural changes in the chromophore environment and there may induce significant changes in the fluorescent signal. Usually, changes in fluorescence in the sensors based on permuted variants of GFP are consequences of changes in ratios of protonated and charged forms of FP chromophore (Fig. 4), which are combined (in some cases) with altered quantum yield of fluorescence for these two forms.

It should be noted that fluorescence photoactivation of PA-GFP [3] and PS-CFP [6] employs the same mechanism; for these proteins the dynamic range of the changed form of a chromophore reaches 100- and 400-fold, respectively (even without consideration of fluorescence quenching of their protonated forms). This suggests a possibility for the development of contrast GES based on cpFPs. Now the maximal dynamic range of such GES has reached 16.5-fold (for the calcium sensor Case 16, see below and Table 4).

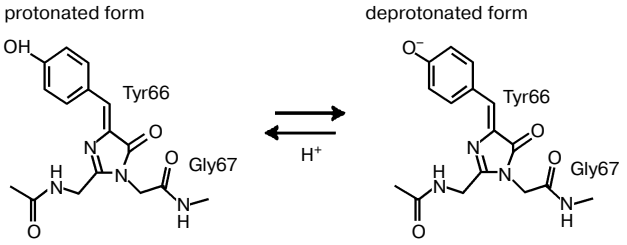

Fig. 4. Transition of the GFP from a neutral (protonated) form (absorbance peak at 400 nm) into the charged (deprotonated) form (absorbance peak at 490 nm).

However, such approach for the development of GES has evident shortcomings. In cpFPs, the chromophore is more exposed into external medium compared with intact FP molecules. This explains relatively low pH stability of cpFP-based indicators. Usually pK_a

Table 4. Comparative characteristics of indicators based on a single FP

Name of sensor	Sensitive domains	cpFP variant	Maximal contrast *in vitro*, fold	Reference
Calcium sensitive indicators based on CaM insertion to EYFP				
Camgaroo-1	CaM	Split EYFP	↑ 7.0	[67]
Camgaroo-2	CaM	Split EYFP(Q69M)	↑ 7.0	[37]
Calcium sensitive indicators based on cpFP				
G-CaMP	M13/CaM	cpEGFP149-144	↑ 4.3	[68]
G-CaMP1.6	M13/CaM(E140K)	mut cpEGFP149-144	↑ 4.9	[70]
Flash-Pericam	M13/CaM(E140Q)	cpEYFP145-144 (Y203H)	↑ 8.0	[71]
Split-Pericam	M13/CaM(E140Q)	cpEYFP145-144 (Y203H)	↑ <8.0	[71]
Ratiometric-Pericam	M13/CaM(E140Q)	cpEYFP145-144 (H148D/Y203F)	↑ 10.0	[71]
Inverse-Pericam	M13/CaM(E140Q)	cpEYFP145-144 (H148T)	↓ 6	[71]
Case12	M13/CaM	cpEYFP145-144(H148E/145T/Y203F)	↑ 12.0	–
Case16	M13/CaM	cpEYFP145-144 (H148E/145S/Y203F)	↑ 16.5	–
Sensor of IR kinase activity based on cpFP				
Cyan-Sinphos	substrate IR/SH2n	cpECFP	↓ >1.1	[72]
Green-Sinphos	substrate IR/SH2n	cpEGFP	↑ >1.15	[72]
Yellow-Sinphos	substrate IR/SH2n	cpCitrine	↑ >1.15	[72]
H_2O_2 sensor based on cpFP				
HyPer	$OxyR_{reg}$	cpEYFP	↑ 2.5	[73]

(pH value at which fluorescence brightness is half of maximal value) is <7.0. Thus, fluorescent properties of such GES depend on the physiological range of pH values. Nevertheless, creation of chimeric constructs based on permuted FPs and sensitive domains (or insertions of FPs inside the sensitive domains) is one of the most promising approaches of the development of genetically encoded fluorescent indicators.

Calcium indicators based on cpFP. In 1999, Baird and coauthors demonstrated that EYFP permuted at position 145 retained its fluorescence. Inserting calmodulin in place of Tyr145, they obtained the calcium indicator named Camgaroo-1 [68]. Formally it was based on the non-permuted form of EYFP (Fig. 5a). However, in reality this sensor is a derivate of permuted variant and therefore is considered in this section.

Excitation spectra of both calcium loaded and calcium free forms of Camgaroo-1 are characterized by a single maximum at 490 nm. In contrast to some below considered permuted variants of FB, the protonated form of cpEYFP, which absorbs at 400 nm, does not exhibit fluorescence. The K_d value for Camgaroo-1 was 7 μM without pronounced bend point for low and high affinity binding sites known for calmodulin. Calcium dependent conformational changes of calmodulin initiated deprotonation of Camgaroo-1 chromophore; this caused a 7-fold increase in the brightness of its fluorescence *in vitro*. The sensor Camgaroo-2 was obtained by the substitution Q69M in the microenvironment of the Camgaroo-1 chromophore [37]. Camgaroo-2 is characterized by insensitivity to chloride ion, lower pK_a value (5.7), higher (2-fold) photostability, and improved expression in organelles and brightness at 37°C. However, due to low affinity these indicators cannot be used for detection of most physiological calcium oscillations, which usually do not exceed 0.1 μM.

Subsequently developed G-CaMP sensor [69] is a calcium GES with significantly improved sensitivity. This indicator is based on EGFP permuted by its 145 position (cpEGFP 149-144), CaM, and its target peptide M13 attached to the C- and N-termini of the permutant, respectively (Fig. 5b). It was demonstrated that this chimeric protein possesses fluorescence, and the intensity of the reversible fluorescence changes in the presence/absence of calcium ions due to interaction between CaM and M13 lead to changes in the chromophore microenvironment accompanied by changes in its fluorescent properties. Addition of calcium ions caused maximal 4.5-fold increase in fluorescence of G-CaMP *in vitro*. The K_d value for G-CaMP was 235 nM; this is about 30 times lower than for Camgaroo. G-CaMP was used for functional analysis of *Drosophila* neurons, but it showed low fluorescence brightness, high pH dependence, and poor maturation at 37°C [70].

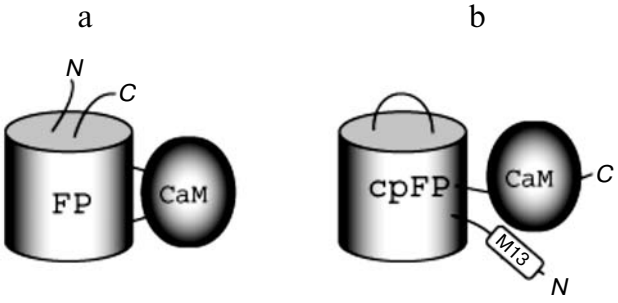

Fig. 5. Scheme of genetically encoded sensors based on one fluorescent protein. a) Calmodulin (CaM) insertion in the EYFP sequence of the calcium indicator Camgaroo. b) Scheme of calcium sensors (type G-Camp, Pericams) based on the permuted variant of FP (cpFP), CaM, and its target peptide M13.

G-GaMP1.6 is an improved version of the G-GaMP sensor. G-CaMP1.6 is significantly brighter than the initial G-CaMP due to increased quantum yield of fluorescence. G-CaMP1.6 also exhibits higher pH stability and improved selectivity with respect to bivalent cations. G-CaMP1.6 exhibits somewhat higher affinity for calcium (K_d = 146 nM) than G-CaMP, and the maximal contrast *in vitro* is 4.9-fold. High signal/noise ratio is the major advantage of G-CaMP1.6, but it (as well as G-CaMP) also demonstrates poor maturation at 37°C [71].

The calcium sensor Pericam was developed using a similar principle [72]. This indicator is based on EYFP permuted by its 145 position (cpEYFP 145-144), M13 was attached to the new N-end, and CaM (E140Q) was attached to the C-end. (Transposition of CaM and M13 resulted in formation of a chimeric protein insensitive to calcium.) Using mutations at positions 148 and 203 (from chromophore environment) three new types of calcium indicators were obtained: Flash-Pericam, Ratiometric-Pericam, and Inverse-Pericam. Binding of calcium ions with Flash-Pericam (Y203H) *in vitro* was accompanied by 8-fold increase in the intensity of its fluorescence. Affinity of Flash-Pericam (K_d = 700 nM) was lower than that of G-CaMP (K_d = 235 nM), but exceeded it in dynamic range. In the absence of calcium, Flash-Pericam exhibited an absorbance spectrum similar to that of cpEYFP, whereas its calcium-bound form was characterized by the increase in absorbance peak at 490 nm and simultaneous decrease in the peak at 400 nm. This suggests that interaction of calcium-bound calmodulin with M13 caused chromophore deprotonation. Flash-Pericam was also characterized by low pH stability and slow maturation at 37°C [72].

In permuted variants of EYFP containing cpEYFP (as in the indicator Flash-Pericam), the protonated form of the chromophore absorbing at 400 nm does not exhibit fluorescence. For the development of two-wavelength (by excitation) calcium indicator, EYFP His203 was mutated for Phe. In contrast to Flash-Pericam, the resultant Ratiometric-Pericam (H148D/Y203F) exhibited two peaks of excitation fluorescence spectrum with maxima at 415 and 494 nm. Addition of calcium ions

caused redistribution in the ratio of fluorescence maxima with dominance of the peak at 494 nm. *In vitro* there was about a 10-fold change in the ratio of brightness of green fluorescence excited at 494 and 415 nm after calcium ion addition. The ratio of excitation peaks (494/415) directly depended on calcium concentration (K_d = 1.7 μM). In contrast to the single wavelength sensors (Flash-Pericam and Inverse-Pericam), redistribution of excitation peaks of fluorescence in Ratiometric-Pericam avoids various artifacts related to indicator concentrations, motility, or cell "thickness" [72].

The calcium-bound form of Inverse-Pericam (H148T) demonstrated *in vitro* a 6-fold decrease in the intensity of green fluorescence emission compared with the calcium free form. Calcium binding did not influence the protonated state of the Inverse-Pericam chromophore, and the decrease in fluorescence emission occurred due to the decrease in quantum yield of fluorescence after binding of calcium ions. The advantage of the Inverse-Pericam indicator consists in its high molar extinction coefficient and quantum yield of fluorescence at pH 7.4, which are characteristic for the calcium free form. Inverse-Pericam has higher affinity for calcium ions (K_d = 0.2 μM) than Flash-Pericam (K_d = 0.7 μM). In contrast to the two other Pericam variants, Inverse-Pericam is less pH sensitive. Thus, in spite of unusual property of fluorescence quenching in the presence of calcium ions, Inverse-Pericam can be used for monitoring of intracellular calcium concentrations with reasonable signal/noise ratio [72].

Significant progress in the development of calcium indicators based on cpFP, M13, and CaM domain has been demonstrated in our recent study (in press). Resultant high contrast calcium indicators are hybrid variants of the above described Ratiometric-Pericam sensors (fluorescent permuted cpYFP (203F)) core and G-CaMP (linker sites, M13 and CaM domains). They differ from their precursors by key positions (145 and 148) of amino acid residues in the chromophore microenvironment. The most contrasting sensors named Case 12 and Case 16 are characterized by maximal (among all GES) dynamic range reaching *in vitro* 12- and 16.5-fold, respectively (Table 4). The new calcium indicators exhibit increased stability, and this property makes them more reliable tools for fluorescent microscopy *in vivo*, comparable with commercially available chemical calcium indicators.

cpFP based sensor for insulin receptor (IR) kinase activity. Protein phosphorylation regulates various processes including protein–protein interactions, protein translocation, and oscillations of second messenger concentrations (calcium, phospholipids metabolites, cyclic nucleotides, etc.). So simultaneous monitoring of several intracellular processes is preferential in studies of mechanisms of signal transduction.

The existing methods for *in vivo* visualization of activity of kinases involved in intracellular signal transductions are mainly based on the FRET approach and require measurements of intensity of fluorescence emission at two wavelengths. Thus, using this approach it is difficult to use fluorescent indicators for parallel measurement of protein phosphorylation and other signaling processes (e.g. protein translocation or changes in second messenger concentrations).

To overcome this problem Kawai and coauthors developed a series of sensors named Sinphos (**sin**gle color fluorescent indicators for protein **phos**phorylation). These sensors can detect kinase activity of insulin receptor (IR) [73]. In contrast to the above-considered FRET based indicators of kinase activity, Sinphos employs fluorescence of only one fluorescent protein. These sensors consist of a peptide tyrosine phosphorylation substrate for IR, permuted variant of a fluorescent protein (cpFP), and the SH2n domain recognizing phosphotyrosine. Depending on permuted cp variants (cpECFP, cpEGFP, or cpCitrine), these indicators were named Cyan, Green, and Yellow Sinphos, respectively. In Sinphos indicators phosphorylation of the substrate domain induces its interaction with phosphoamino acid recognizing domain followed by subsequent conformational rearrangements of cpFP and change in intensity of its fluorescence.

It was demonstrated that during insulin stimulation of CHO-IR cells Cyan-Sinphos showed 10% decrease in fluorescence intensity, whereas Green and Yellow-Sinphos indicators demonstrated 15% increase in fluorescence intensity. Such difference in fluorescence intensity can be attributed to differences in chromophore structure of these indicators. It is known that the cpEGFP chromophore can exist in both protonated and deprotonated states. The increase in fluorescence intensity of Green-Sinphos in response to phosphorylation is determined by deprotonation of its chromophore; this occurs during interaction of SH2n domain with phosphotyrosine. The cpECFP is totally deprotonated and so binding of SH2n with Cyan-Sinphos phosphotyrosine does not influence its state. The decrease in fluorescence of Cyan-Sinphos in response to IR phosphorylation is determined by the decrease in quantum yield of its fluorescence, which occurs as a result of structural rearrangements of the chromophore. On the other hand, Yellow-Sinphos fluorescence intensity depends not only on phosphorylation but on other factors as well (e.g. intracellular pH value) [73].

Application of the Sinphos indicators based on only one chromophore allowed simultaneous visualization of two insulin-induced processes: IR protein phosphorylation and translocation of ERK kinase. CHO-IR cells were cotransfected with the indicator Cyan-Sinphos and CFP tagged mitogen activated ERK kinase, and also MAPK kinase required for cytoplasmic localization of ERK in unstimulated cells. Stimulation of cells with insulin caused a decrease in Cyan-Sinphos fluorescence intensity; this suggested activation of IR kinase activity. Besides this activation, there was migration of GFP-ERK from

the cytoplasm into the nucleus attributed to dissociation of this enzyme from MAPKK. This demonstrates that the Sinphos indicators can be successfully used in combination with fluorescently labeled proteins and also with chemiluminescent dyes and fluorescent indicators based on a fluorescent protein of different color. Kinase specificity of Sinphos can be changed by substitution of substrate and phosphoamino acid recognizing domains. Thus, it is possible to monitor simultaneously two kinase processes using two Sinphos variants with different kinase selectivity and fluorescence color [73].

H_2O_2 sensor based on cpFP. In 2006, a GES for H_2O_2 was constructed in our laboratory [74]. This indicator named HyPer (from **h**ydrogen **per**oxide) consists of the permuted variant of EYFP (cpEYFP) inserted into the regulatory domain of prokaryotic OxyR protein sensitive to hydrogen peroxide. Interaction of HyPer with H_2O_2 causes oxidation of two cysteine residues of OxyR causing significant conformational changes. This results in conformational changes of the permuted core of the sensor accompanied by changes of its fluorescent properties. The mechanism of HyPer action is similar to the above-described mechanism of functioning of the calcium sensor Ratiometric-Pericam. The peak of fluorescence excitation at 420 nm proportionally decreased with the increase of the peak at 500 nm. This suggests chromophore deprotonation. As most sensors based on permuted variants of GFP, the HyPer fluorescence also depends on pH. The pH titration curve for HyPer is almost identical to that of Ratiometric-Pericam [74].

HyPer is characterized by high sensitivity and selectivity with respect to hydrogen peroxide, reversibility of response, and lack of interaction with the biochemical environment of the cell due to use of the OxyR bacterial detector domain. Using this sensor, it was possible to detect submicromolar oscillations of intracellular hydrogen peroxide in the cytoplasm and mitochondria of cells during apoptosis and growth factor stimulation. Maximal change in fluorescence was 2.5-fold.

Latest innovations in the field of intracellular measurement *in vivo* are based on use of GES changing their fluorescent properties in response to various intracellular signals or analytes. These GES can be directed to a particular cell compartment or to a certain type of tissues of transgenic organisms. They are used in both basic research and high throughput drug screenings and in some cases they have already replaced synthetic indicators.

During recent decades, many molecular sensors of various specificities have been developed on the basis of FPs. However, in most cases their dynamic range cannot reliably characterize intracellular processes. One of the most promising approaches in design of GES is based on permuted FPs; however, application of the existing variants is limited by their high pH sensitivity.

Thus, the development of effective genetically encoded fluorescent sensors, combining high pH stability, high dynamic range, high brightness, and photostability still represents an important direction in modern studies. High activity of studies on the engineering GES gives hope for significant progress in the field during coming years.

REFERENCES

1. Labas, Y. A., Gurskaya, N. G., Yanushevich, Y. G., Fradkov, A. F., Lukyanov, K. A., Lukyanov, S. A., and Matz, M. V. (2002) *Proc. Natl. Acad. Sci. USA*, **99**, 4256-4261.
2. Chudakov, D. M., Lukyanov, S., and Lukyanov, K. A. (2005) *Trends Biotechnol.*, **23**, 605-613.
3. Patterson, G. H., and Lippincott-Schwartz, J. (2002) *Science*, **297**, 1873-1877.
4. Ando, R., Hama, H., Yamamoto-Hino, M., Mizuno, H., and Miyawaki, A. (2002) *Proc. Natl. Acad. Sci. USA*, **99**, 12651-12656.
5. Lukyanov, K. A., Chudakov, D. M., Lukyanov, S., and Verkhusha, V. V. (2005) *Nat. Rev. Mol. Cell. Biol.*, **6**, 885-891.
6. Chudakov, D. M., Verkhusha, V. V., Staroverov, D. B., Souslova, E. A., Lukyanov, S., and Lukyanov, K. A. (2004) *Nat. Biotechnol.*, **22**, 1435-1439.
7. Chudakov, D. M., Belousov, V. V., Zaraisky, A. G., Novoselov, V. V., Staroverov, D. B., Zorov, D. B., Lukyanov, S., and Lukyanov, K. A. (2003) *Nat. Biotechnol.*, **21**, 191-194.
8. Chudakov, D. M., Chepurnykh, T. V., Belousov, V. V., Lukyanov, S., and Lukyanov, K. A. (2006) *Traffic*, **7**, 1304-1310.
9. Gurskaya, N. G., Verkhusha, V. V., Shcheglov, A. S., Staroverov, D. B., Chepurnykh, T. V., Fradkov, A. F., Lukyanov, S., and Lukyanov, K. A. (2006) *Nat. Biotechnol.*, **24**, 461-465.
10. Lippincott-Schwartz, J., Altan-Bonnet, N., and Patterson, G. H. (2003) *Nat. Cell. Biol.*, Suppl., S7-S14.
11. Jares-Erijman, E. A., and Jovin, T. M. (2006) *Curr. Opin. Chem. Biol.*, **10**, 409-416.
12. Schultz, C., Schleifenbaum, A., Goedhart, J., and Gadella, T. W., Jr. (2005) *Chembiochem.*, **6**, 1323-1330.
13. Cabantous, S., Terwilliger, T. C., and Waldo, G. S. (2005) *Nat. Biotechnol.*, **23**, 102-107.
14. Yan, D., Guo, L., and Wang, Y. (2006) *J. Cell. Biol.*, **174**, 415-424.
15. Terskikh, A., Fradkov, A., Ermakova, G., Zaraisky, A., Tan, P., Kajava, A. V., Zhao, X., Lukyanov, S., Matz, M., Kim, S., Weissman, I., and Siebert, P. (2000) *Science*, **290**, 1585-1588.
16. Verkhusha, V. V., Chudakov, D. M., Gurskaya, N. G., Lukyanov, S., and Lukyanov, K. A. (2004) *Chem. Biol.*, **11**, 845-854.
17. Robey, R. B., Ruiz, O., Santos, A. V., Ma, J., Kear, F., Wang, L. J., Li, C. J., Bernardo, A. A., and Arruda, J. A. (1998) *Biochemistry*, **37**, 9894-9901.
18. Miesenbock, G., de Angelis, D. A., and Rothman, J. E. (1998) *Nature*, **394**, 192-195.
19. Kneen, M., Farinas, J., Li, Y., and Verkman, A. S. (1998) *Biophys. J.*, **74**, 1591-1599.
20. Hanson, G. T., McAnaney, T. B., Park, E. S., Rendell, M. E., Yarbrough, D. K., Chu, S., Xi, L., Boxer, S. G., Montrose, M. H., and Remington, S. J. (2002) *Biochemistry*, **41**, 15477-15488.

21. McAnaney, T. B., Park, E. S., Hanson, G. T., Remington, S. J., and Boxer, S. G. (2002) *Biochemistry*, **41**, 15489-15494.
22. Wachter, R. M., and Remington, S. J. (1999) *Curr. Biol.*, **9**, R628-629.
23. Jayaraman, S., Haggie, P., Wachter, R. M., Remington, S. J., and Verkman, A. S. (2000) *J. Biol. Chem.*, **275**, 6047-6050.
24. Barondeau, D. P., Kassmann, C. J., Tainer, J. A., and Getzoff, E. D. (2002) *J. Am. Chem. Soc.*, **124**, 3522-3524.
25. Li, Y., Agrawal, A., Sakon, J., and Beitle, R. R. (2001) *J. Chromatogr. A*, **909**, 183-190.
26. Zubova, N. N., and Savitsky, A. P. (2005) *Usp. Biol. Khim.*, **45**, 391-455.
27. Gu, Y., Di, W. L., Kelsell, D. P., and Zicha, D. (2004) *J. Microsc.*, **215**, 162-173.
28. Rizzo, M. A., and Piston, D. W. (2005) *Biophys. J.*, **88**, L14-16.
29. Van Munster, E. B., and Gadella, T. W. (2005) *Adv. Biochem. Eng. Biotechnol.*, **95**, 143-175.
30. Harpur, A. G., Wouters, F. S., and Bastiaens, P. I. (2001) *Nat. Biotechnol.*, **19**, 167-169.
31. Miyawaki, A. (2003) *Dev. Cell*, **4**, 295-305.
32. Berridge, M. J. (1998) *Neuron*, **21**, 13-26.
33. Romoser, V. A., Hinkle, P. M., and Persechini, A. (1997) *J. Biol. Chem.*, **272**, 13270-13274.
34. Miyawaki, A., Llopis, J., Heim, R., McCaffery, J. M., Adams, J. A., Ikura, M., and Tsien, R. Y. (1997) *Nature*, **388**, 882-887.
35. Porumb, T., Yau, P., Harvey, T. S., and Ikura, M. (1994) *Protein Eng.*, **7**, 109-115.
36. Miyawaki, A., Griesbeck, O., Heim, R., and Tsien, R. Y. (1999) *Proc. Natl. Acad. Sci. USA*, **96**, 2135-2140.
37. Griesbeck, O., Baird, G. S., Campbell, R. E., Zacharias, D. A., and Tsien, R. Y. (2001) *J. Biol. Chem.*, **276**, 29188-29194.
38. Mizuno, H., Sawano, A., Eli, P., Hama, H., and Miyawaki, A. (2001) *Biochemistry*, **40**, 2502-2510.
39. Truong, K., Sawano, A., Mizuno, H., Hama, H., Tong, K. I., Mal, T. K., Miyawaki, A., and Ikura, M. (2001) *Nat. Struct. Biol.*, **8**, 1069-1073.
40. Nagai, T., Yamada, S., Tominaga, T., Ichikawa, M., and Miyawaki, A. (2004) *Proc. Natl. Acad. Sci. USA*, **101**, 10554-10559.
41. Nagai, T., Ibata, K., Park, E. S., Kubota, M., Mikoshiba, K., and Miyawaki, A. (2002) *Nat. Biotechnol.*, **20**, 87-90.
42. Matz, M. V., Fradkov, A. F., Labas, Y. A., Savitsky, A. P., Zaraisky, A. G., Markelov, M. L., and Lukyanov, S. A. (1999) *Nat. Biotechnol.*, **17**, 969-973.
43. Heim, N., and Griesbeck, O. (2004) *J. Biol. Chem.*, **279**, 14280-14286.
44. Mank, M., Reiff, D. F., Heim, N., Friedrich, M. W., Borst, A., and Griesbeck, O. (2006) *Biophys. J.*, **90**, 1790-1796.
45. Kohl, S., Marx, T., Giddings, I., Jagle, H., Jacobson, S. G., Apfelstedt-Sylla, E., Zrenner, E., Sharpe, L. T., and Wissinger, B. (1998) *Nat. Genet.*, **19**, 257-259.
46. Zaccolo, M., de Giorgi, F., Cho, C. Y., Feng, L., Knapp, T., Negulescu, P. A., Taylor, S. S., Tsien, R. Y., and Pozzan, T. (2000) *Nat. Cell Biol.*, **2**, 25-29.
47. Honda, A., Adams, S. R., Sawyer, C. L., Lev-Ram, V., Tsien, R. Y., and Dostmann, W. R. (2001) *Proc. Natl. Acad. Sci. USA*, **98**, 2437-2442.
48. Sato, M., Hida, N., Ozawa, T., and Umezawa, Y. (2000) *Analyt. Chem.*, **72**, 5918-5924.
49. Nikolaev, V. O., Gambaryan, S., and Lohse, M. J. (2006) *Nat. Meth.*, **3**, 23-25.
50. Janetopoulos, C., Jin, T., and Devreotes, P. (2001) *Science*, **291**, 2408-2411.
51. Mochizuki, N., Yamashita, S., Kurokawa, K., Ohba, Y., Nagai, T., Miyawaki, A., and Matsuda, M. (2001) *Nature*, **411**, 1065-1068.
52. Itoh, R. E., Kurokawa, K., Ohba, Y., Yoshizaki, H., Mochizuki, N., and Matsuda, M. (2002) *Mol. Cell Biol.*, **22**, 6582-6591.
53. Hoffman, G. R., Nassar, N., and Cerione, R. A. (2000) *Cell*, **100**, 345-356.
54. Seth, A., Otomo, T., Yin, H. L., and Rosen, M. K. (2003) *Biochemistry*, **42**, 3997-4008.
55. Yoshizaki, H., Ohba, Y., Kurokawa, K., Itoh, R. E., Nakamura, T., Mochizuki, N., Nagashima, K., and Matsuda, M. (2003) *J. Cell Biol.*, **162**, 223-232.
56. Hagiwara, M., Brindle, P., Harootunian, A., Armstrong, R., Rivier, J., Vale, W., Tsien, R., and Montminy, M. R. (1993) *Mol. Cell Biol.*, **13**, 4852-4859.
57. Ng, T., Squire, A., Hansra, G., Bornancin, F., Prevostel, C., Hanby, A., Harris, W., Barnes, D., Schmidt, S., Mellor, H., Bastiaens, P. I., and Parker, P. J. (1999) *Science*, **283**, 2085-2089.
58. Lee, T., and Luo, L. (1999) *Neuron*, **22**, 451-461.
59. Nagai, Y., Miyazaki, M., Aoki, R., Zama, T., Inouye, S., Hirose, K., Iino, M., and Hagiwara, M. (2000) *Nat. Biotechnol.*, **18**, 313-316.
60. Zhang, J., Ma, Y., Taylor, S. S., and Tsien, R. Y. (2001) *Proc. Natl. Acad. Sci. USA*, **98**, 14997-15002.
61. Ting, A. Y., Kain, K. H., Klemke, R. L., and Tsien, R. Y. (2001) *Proc. Natl. Acad. Sci. USA*, **98**, 15003-15008.
62. Kurokawa, K., Mochizuki, N., Ohba, Y., Mizuno, H., Miyawaki, A., and Matsuda, M. (2001) *J. Biol. Chem.*, **276**, 31305-31310.
63. Sasaki, K., Sato, M., and Umezawa, Y. (2003) *J. Biol. Chem.*, **278**, 30945-30951.
64. Kunkel, M. T., Ni, Q., Tsien, R. Y., Zhang, J., and Newton, A. C. (2005) *J. Biol. Chem.*, **280**, 5581-5587.
65. Violin, J. D., Zhang, J., Tsien, R. Y., and Newton, A. C. (2003) *J. Cell Biol.*, **161**, 899-909.
66. Green, H. M., and Alberola-Ila, J. (2005) *BMC Chem. Biol.*, **5**, 1.
67. Heinemann, U., and Hahn, M. (1995) *Progr. Biophys. Mol. Biol.*, **64**, 121-143.
68. Baird, G. S., Zacharias, D. A., and Tsien, R. Y. (1999) *Proc. Natl. Acad. Sci. USA*, **96**, 11241-11246.
69. Nakai, J., Ohkura, M., and Imoto, K. (2001) *Nat. Biotechnol.*, **19**, 137-141.
70. Wang, L., Jackson, W. C., Steinbach, P. A., and Tsien, R. Y. (2004) *Proc. Natl. Acad. Sci. USA*, **101**, 16745-16749.
71. Ohkura, M., Matsuzaki, M., Kasai, H., Imoto, K., and Nakai, J. (2005) *Analyt. Chem.*, **77**, 5861-5869.
72. Nagai, T., Sawano, A., Park, E. S., and Miyawaki, A. (2001) *Proc. Natl. Acad. Sci. USA*, **98**, 3197-3202.
73. Kawai, Y., Sato, M., and Umezawa, Y. (2004) *Analyt. Chem.*, **76**, 6144-6149.
74. Belousov, V. V., Fradkov, A. F., Lukyanov, K. A., Staroverov, D. B., Shakhbazov, K. S., Terskikh, A. V., and Lukyanov, S. (2006) *Nat. Meth.*, **3**, 281-286.